Acta Crystallographica Section D
Biological Crystallography
ISSN 0907-4449

Avian haemoglobins and structural basis of high affinity for oxygen: structure of bar-headed goose aquomet haemoglobin

Xiao-Zhou Liu, Song-Lin Li,† Hua Jing,‡ Yu-He Liang, Zi-Qian Hua and Guang-Ying Lu*

National Laboratory of Protein Engineering and Plant Genetic Engineering, College of Life Sciences, Peking University, Beijing 100871, People's Republic of China

† Present address: Department of Microbiology, University of Alabama at Birmingham, Birmingham, AL 35294-2041, USA.
‡ Present address: Center for Blood Research, Harvard Medical School, Boston, MA 02115, USA.

Correspondence e-mail: lugy@pku.edu.cn

Received 18 October 2000
Accepted 8 March 2001

PDB Reference: bar-headed goose aquomet Hb, 1c40.

Haemoglobin from the bar-headed goose (*Anser indicus*) has higher oxygen affinity than that from its lowland relatives such as greylag goose (*A. anser*). The crystal structure of bar-headed goose aquomet haemoglobin was determined at 2.3 Å resolution and compared with the structures of the goose oxy, human, horse and other avian haemoglobins and the sequences of other avian haemoglobins. Four amino-acid residues differ between greylag goose and bar-headed goose haemoglobins, among which Alaα119 and Aspβ125 in bar-headed goose haemoglobin reduces the contacts between the α_1 and β_1 subunits compared with Pro and Glu, respectively, and therefore may increase the oxygen affinity by loosening the $\alpha_1\beta_1$ interface. Compared with human oxy haemoglobin, the relative orientation of two $\alpha\beta$ dimers in the bar-headed goose aquomet and oxy Hbs are rotated by about 4°, indicating a unique quaternary structural difference from the typical R state. This new 'R_H' state is probably correlated with the higher oxygen affinity of bar-headed goose haemoglobin.

1. Introduction

The bar-headed goose (*A. indicus*) is one of the most successful vertebrates to survive and reproduce at high altitude. It lives in central Asia and Qinghai Lake in China at an altitude of 4000–6000 m, but migrates in late autumn to the plains of northwest India, during which it flies over the Himalayas, ~9000 m in altitude. In contrast to its lowland relatives such as the greylag goose (*A. anser*), the bar-headed goose can even tolerate short exposure to at least 10 700 m (Black & Tenny, 1980; Swan, 1970). Therefore, it has long been considered a favourable subject for studying the mechanism of high-altitude hypoxia respiration. In addition to physiological factors, the ability of the bar-headed goose to tolerate extremely hypoxic conditions is attributed to the increased oxygen affinity of its haemoglobin (Hb) (Petschow *et al.*, 1977; Rollema & Bauer, 1979). In the absence of inositol pentaphosphate (IPP), an allosteric regulator of avian Hb, the oxygen affinity of the bar-headed goose Hb is slightly higher (P_{50} = 0.263 kPa in 100 m*M* Cl^- at pH 7.2, 298 K) than that of greylag goose Hb (P_{50} = 0.368 kPa), whereas in the presence of IPP the difference is much enhanced (P_{50} of 2.684 *versus* 4.066 kPa). The amino-acid sequences of the major Hb of these two species differ at four positions, Gly (greylag) *versus* Ser (bar-headed goose) at α18, Ala *versus* Val at α63, Pro *versus* Ala at α119 and Glu *versus* Asp at β125 (Oberthur *et al.*, 1981). To identify the effects of these differences on the Hb structure and to elucidate the structural basis of high oxygen affinity, we determined the structure of bar-headed goose

Table 1
Data and structure statistics.

Data statistics	
No. of observations	28271
No. of unique reflections	15792
Resolution (Å)	26.87–2.3
Completeness (overall) (%)	95.2
Completeness (2.3–2.41 Å) (%)	70.1
Data with $I > 2\sigma(I)$ (overall) (%)	93.1
Data with $I > 2\sigma(I)$ (2.3–2.43 Å) (%)	87.8
$R_{\rm merge}$† (overall) (%)	7.2
Multiplicity (overall)	2.66
Multiplicity (2.3–2.43 Å)	1.84
Structure statistics	
R factor‡ (%)	19.8
$R_{\rm free}$§ (%)	24.7
No. of non-H atoms	2241
No. of atoms in haem	88
No. of water molecules	60
R.m.s. deviation from ideality	
Bond lengths (Å)	0.010
Bond angles (°)	1.40
Dihedral angles (°)	19.3
Improper angles (°)	1.18

† $R_{\rm merge} = \sum_h \sum_i |I_i - \langle I\rangle| / \sum_h \sum_i I_i$, where I_i is the measured intensity for reflection i and $\langle I\rangle$ is the mean intensity. ‡ R factor $= \sum_h ||F_o| - k|F_c|| / \sum_h |F_o|$, where F_o and F_c are the observed and calculated structure factors, respectively. § R factor calculated for 6.9% of total reflections that were always excluded in refinement.

aquomet Hb and compared it with some relevant Hb structures.

The Hb molecule consists of two α- and two β-subunits arranged in pseudo-222 symmetry. The quaternary structure changes allosterically in response to ligand binding, generating the R state (relaxed, liganded) or T state (tense, ligand-free). The $\alpha_1\beta_1$ interface (packing interface) and the $\alpha_1\beta_2$ interface (sliding interface) are crucial to the oxygen affinity and the allosteric transition between the R and T states, respectively (Perutz *et al.*, 1987). The Proα119 (greylag goose) to Alaα119 (bar-headed goose) mutation was predicted to eliminate a van der Waals contact with Leuβ55 in the $\alpha_1\beta_1$ interface (Oberthur, Brauneitzer *et al.*, 1982); the reduction of the van der Waals contact can loosen the $\alpha_1\beta_1$ interface, thereby destabilizing the T state with low oxygen affinity and favouring the R state with high oxygen affinity (Perutz, 1983; Perutz *et al.*, 1987; Hiebl *et al.*, 1987). Therefore, it was speculated that the high oxygen affinity of bar-headed goose Hb and the mechanism of hypoxia adaptation mainly arise from the loosening of the $\alpha_1\beta_1$ interface (Oberthur, Brauneitzer *et al.*, 1982; Perutz, 1983; Perutz *et al.*, 1987; Hiebl *et al.*, 1987). The Pro$\rightarrow$Alaα119 and Met$\rightarrow$Serβ55 mutations were introduced individually into human Hb by protein engineering; increased oxygen affinities were observed for the two mutants at a level similar to that on going from greylag goose Hb to bar-headed goose Hb (Jessen *et al.*, 1991; Weber *et al.*, 1993). How such amino-acid differences affect the tertiary and quaternary structure of Hb and thereby its oxygen affinity can be answered by studying the structure of bar-headed goose Hb and its differences from the Hbs of lowland animals.

Of all the Hb structures previously solved, only two are avian Hbs. One is the structure of bar-headed goose oxy Hb determined previously in our laboratory (Zhang *et al.*, 1996) and the other is the structure of chicken HbD, which is a minor component of adult chicken Hb (Knapp *et al.*, 1999). The structure of the bar-headed goose oxy Hb supports the speculation on the role of α119 mentioned above. Here, the structure of bar-headed goose aquomet Hb is presented in which the haem iron Fe^{2+} is oxidized to Fe^{3+} and the ligand oxygen is replaced by a water molecule. This met Hb form was stable and the easiest to obtain experimentally. The aquomet Hb structure was analyzed in detail and compared with the bar-headed goose oxy Hb, human oxy Hb, horse aquomet Hb and chicken HbD structures. The study revealed a unique quaternary structure feature for the liganded bar-headed goose Hb and critical roles for two amino-acid differences at α119 and β125 between bar-headed goose and greylag goose Hbs, both of which may contribute to the higher oxygen affinity.

2. Materials and methods

2.1. Crystallization and data collection

The bar-headed goose aquomet Hb was prepared, purified and crystallized as described previously (Lu *et al.*, 1989). Briefly, red blood cells were prepared from blood drawn from the vein of a bar-headed goose, washed with 0.82% NaCl and lysed with the same volume of distilled water. Cell membranes and other insoluble materials were removed by adding half a volume of CCl_4, shaking and centrifuging at 4000 rev min^{-1} for 20 min. Solid $K_3Fe(CN)_6$ powder was added to the supernatant solution containing Hb at 33.3 mg ml^{-1}. The mixture was stirred for 10 min and then dialyzed against 10 m*M* NaCl. The sample was further purified on Sephadex-100 with 10 m*M* NaCl as buffer. The purified protein was dialyzed against 5 m*M* potassium phosphate buffer pH 6.8 and concentrated to 50–60 mg ml^{-1}.

Crystals were obtained by the hanging-drop vapour-diffusion method at 291 K. A 10 µl droplet containing 5 µl Hb solution, 2 µl 20% PEG 6000 and 3 µl 50 m*M* potassium phosphate buffer pH 6.8 was equilibrated against 1 ml reservoir solution containing 12% PEG 6000. Crystals can attain maximum dimensions of 0.6 × 0.6 × 0.4 mm in 7–10 d. The crystals belong to space group $P4_22_12$, with unit-cell parameters $a = b = 81.5$, $c = 107.2$ Å. Each asymmetric unit contains half a molecule or one $\alpha\beta$ dimer, which is related to the other half by the crystallographic twofold axis. The $V_{\rm M}$ value is 2.66 Å^3 Da^{-1} and the solvent content is 54%.

Diffraction data were collected at 293 K on a multiwire area detector X-200B (Siemens Co.) using Cu $K\alpha$ radiation (wavelength 1.5418 Å) from a Rigaku RU-300 rotating-anode X-ray generator operated at 250 mA and 50 kV. The crystal-to-detector distance was 154 mm. A total of 714 frames were collected at $2\theta = 20^\circ$, $\chi = 45^\circ$ and ω in the range -20 to 160° with an interval of 0.25°. The exposure time per frame was 120 s. The data were processed with *XENGEN* (Howard *et al.*, 1987). A total of 28 271 observations of 15 782 unique reflections within the 26.87–2.3 Å resolution range were collected with an $R_{\rm merge}$ of 7.2% and a multiplicity of 2.66. The

completeness of the overall data set is 95.2% and the completeness of the highest resolution shell (2.3–2.41 Å) is 70.1%. The data statistics are listed in Table 1.

2.2. Structure determination and refinement

The initial phases were determined by the molecular-replacement method using *AUTOMR* (Matsuura, 1991). The 2.1 Å structure of horse aquomet Hb $\alpha\beta$ dimer (PDB 2mhb; Ladner *et al.*, 1977) was used as the search model; it has a sequence identity of 71.6% with the α-subunit of bar-headed goose Hb and 67.1% with the β-subunit. The model was rotated with arbitrary angles in a spherical polar coordinate system and then placed in an orthogonal cell with dimensions $100 \times 100 \times 100$ Å and $P1$ symmetry. The rotation function was calculated using data in the resolution range 10–4 Å with an integration radius of 25 Å within the spherical polar angles $0 < \psi < 90^\circ$, $0 < \varphi < 360^\circ$, $0 < \chi < 360^\circ$ and with an interval of 5°. The top 20 independent rotation-function solutions were used for translation-function calculations using data in the resolution range 12–8 Å. The top ten independent translation solutions were then used in rigid-body refinement in the 10–4 Å resolution range. The best solution has an R factor of 0.428 and a correlation coefficient of 0.582 and corresponds to the highest peak in the rotation function. The rotation angles and translation vectors were applied to the model and the main chains of the model in the goose aquomet Hb unit cell were plotted. The molecular packing in the crystal lattice is reasonable.

For model rebuilding, the residues in horse Hb were replaced by those in bar-headed goose Hb and the model was adjusted manually based on $2F_o - F_c$ and $F_o - F_c$ maps. The model was then refined and rebuilt for a number of cycles using *CNS* (Brunger *et al.*, 1998) and *XFIT* (McRee, 1992), respectively. An initial model, consisting of 2325 non-H atoms from 287 residues and two haems, was refined. All 15 772 reflections in the resolution range 26.8–2.3 Å were used in the refinement, of which 14 638 reflections were used as the working set and 1084 reflections (6.9%) were used in the test set (Table 1). The initial B factors of all atoms were set to 15 Å^2. The starting temperature in simulated annealing was 2500 K and the cooling rate was 25 K per cycle. Individual B factors were then refined. In each refinement cycle, the weight factor WA estimated by the program was scaled by 0.5 to obtain the lowest $R_{\rm free}$, the refinement target is a maximum-likelihood target and overall anisotropic B-factor correction with a lower resolution limit of 6 Å and bulk-solvent corrections were applied to the data. The model was harmonically restrained during the slow-cool annealing refinement with energy constants of 42 kJ mol^{-1} Å^2 for all C$^\alpha$ and water O atoms and 21 kJ mol^{-1} Å^2 for other atoms, except for nine residues at the N- and C-termini that have poor electron densities. After each refinement cycle, σ_A-weighted $2mF_o - DF_c$ and $mF_o - DF_c$ maps were calculated which guided further manual rebuilding. Water molecules were added in the last few cycles using the automatic water-picking protocol in *CNS* with a cutoff of 1.0σ for the σ_A-weighted $2mF_o - DF_c$ map; if they were within 2.6–4.0 Å of any atom or 2.2–4.0 Å of the O or N atoms then their B factors refined to a value below 50 Å^2. The final R factor is 0.197 and $R_{\rm free}$ is 0.247. The density level of the bulk-solvent model is 0.289 e Å^{-3} and its B factor is 29.7 Å^2. The statistics of the final structure are summarized in Table 1.

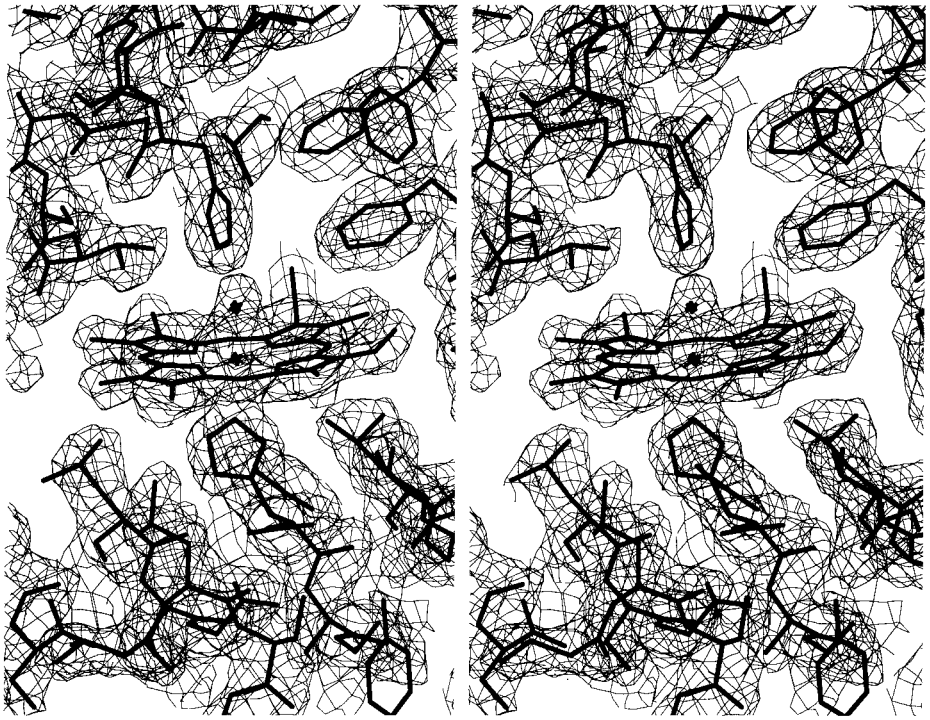

Figure 1
σ_A-weighted $2F_o - F_c$ map around the haem group in the α-subunit of bar-headed goose aquomet Hb.

2.3. Structure analysis and comparison

The structures of bar-headed goose aquomet Hb, oxy Hb (PDB code 1a4f; Zhang *et al.*, 1996), chicken HbD (1hbr; Knapp *et al.*, 1999), human oxy Hb (1hho; Shaanan, 1983) and horse aquomet Hb (2mhb; Ladner *et al.*, 1977) were aligned and visually compared using *XTALVIEW* (McRee, 1992). The contacts between the subunits and the quaternary geometry of the tetramers were calculated using *CNS* (Brunger *et al.*, 1998). The fitting frame defined by Zhang *et al.* (1996) was used for calculating the quaternary geometry of the tetramers. The fitting residues are α3–13, 31–42, 54–73, 80–84, 97–104, 117–136 and β26–37, 62–68, 106–114 and 127–139, a total of 117 amino-acid residues and 468 atoms. These account for 40.8% of the main-chain

atoms in the $\alpha\beta$ dimer. The fitting frame is slightly different from that defined by Baldwin & Chothia (1979), in which the $\alpha_1\beta_1$ contact interface was used as the reference region for comparison of different human Hb forms, but structural differences between goose and human Hb make the region used by Baldwin and Chothia less suitable for overlapping the coordinates. The criteria for van der Waals contacting distances are C—C, 4.1 Å; C—N, 3.8 Å; C—O, 3.7 Å; N—N, 3.4 Å; N—O, 3.4 Å; O—O, 3.3 Å (Acqua *et al.*, 1998). The planarity of haem was calculated using *GEOMCALC* from the *CCP*4 program suite (Collaborative Computational Project, Number 4, 1994). The figures were prepared using *XTALVIEW* unless otherwise specified.

3. Results

3.1. Structure quality

The structure contains all 287 residues in the amino-acid sequence, two haems and 60 water molecules (Table 1), all of which fit well to the electron-density map except for the terminal residues Lysα139–Argα141, Valβ1 and Lysβ144–Hisβ146, which have high *B* factors. These terminal regions could be flexible in nature, as also evident from the deviations between different Hb structures (see below). An example electron-density map is shown in Fig. 1 for the region around the haem group of the α-subunit.

The stereochemical quality of the structure as assessed by *PROCHECK* (Laskowski *et al.*, 1993) is excellent (Table 1). In the Ramachandran plot (Ramakrishnan & Ramachandran, 1965), 92.6% of the residues are in the most favoured regions and 7.4% of the residues are in the additionally allowed regions (Fig. 2). The estimated coordinate error from the Luzzati plot (Luzzati, 1952) is 0.27 Å. The average *B* factor is 22.1 Å^2 for all non-H atoms, 19.8 Å^2 for main-chain atoms, 23.9 Å^2 for side-chain atoms and 30.7 Å^2 for water molecules. The average *B* factors for the main-chain and side-chain atoms of each residue in the α-subunit and β-subunit are plotted in Fig. 3.

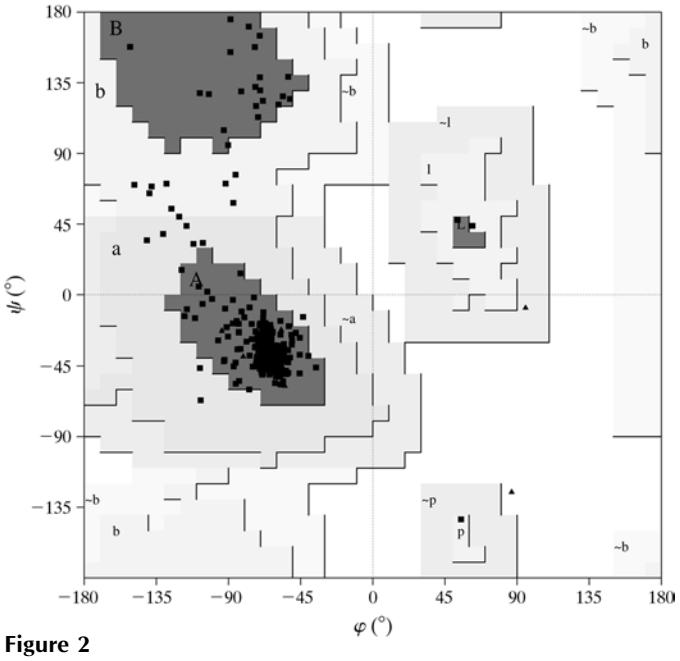

Figure 2
Ramachandran plot for bar-headed goose aquomet Hb, plotted using *PROCHECK* (Laskowski *et al.*, 1993). 92.6% of the residues are in the most favoured regions and 7.4% in the additional allowed regions. The positions of glycines are shown as triangles.

3.2. Subunit structure and quaternary structure

As in other known Hb structures, the α-subunit contains seven helices, *A*–*G*, the β-subunit contains eight helices, *A*–*H*, and the helices are linked by loops which are also called corners. The overall subunit structure of bar-headed goose aquomet Hb superimposes well with the four Hb structures being compared; the RMSDs are listed in Table 2(*a*). The smallest deviation among these structures is obviously that between the bar-headed goose oxy and aquomet Hbs. Their C$^\alpha$ traces are almost identical even though different initial models were used in molecular replacement, suggesting that the two structures converge in refinement and are consistent with each other (Fig. 4). The next smallest difference is between the β-subunits of goose Hb and chicken HbD; this may be attributable to the conservation of β-subunit sequences of avian Hbs. However, the α^D subunit of chicken HbD deviates significantly from the other α^A subunits, indicating that the three-dimensional structure of chicken α^D has larger differences from α^A of the goose, human and horse Hbs. The differences between goose α^A and chicken α^D reside mainly on the *A* helix, the *AB* and *GH* corners and two termini. The largest deviation is between the goose Hb and human or horse Hb. The differences between the goose Hb and human Hb reside mainly on the *B* and *G* helices and the *AB*, *CE* and *GH* corners in the α-subunit, the *A*, *D* and *F* helices and the *CD*, *DE*, *EF* and *GH* corners in the β-subunit and the two termini of each subunit. In general, except for the chicken α^D subunit, the deviations between the β-subunits of goose

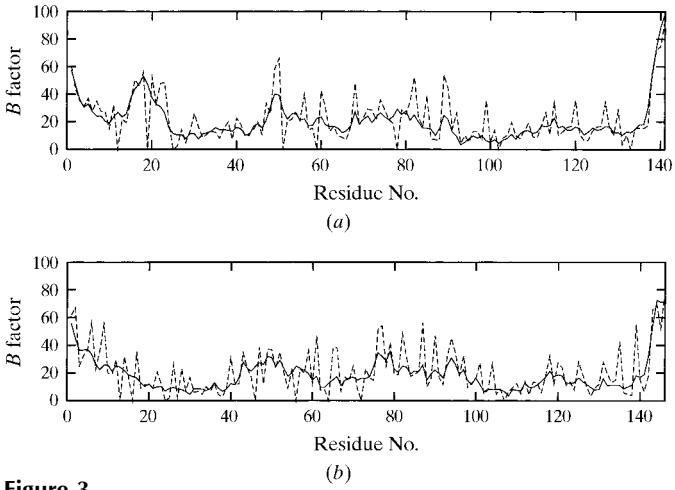

Figure 3
Plot of the average *B* factor (Å^2) for the main-chain (solid line) and side-chain (dashed line) atoms of each residue in the α-subunit (*a*) and β-subunit (*b*).

Table 2
Summary of structure comparisons.

(*a*) RMSD between bar-headed goose aquomet Hb and four other Hb structures.

	Goose oxy Hb	Chicken HbD	Horse met Hb	Human oxy Hb
α-Subunit	0.3508	0.9959	0.6792	0.7188
β-Subunit	0.5347	0.4394	1.1027	0.9748
$\alpha_1\beta_1$ Dimer	0.4569	0.6293	0.9772	0.9366
Tetramer	0.4698	0.7362	1.0404	1.0661

(*b*) Quaternary structural differences from human oxy and deoxy Hbs as measured by rotation and translation of the $\alpha_2\beta_2$ dimer of a tetramer after fitting the $\alpha_1\beta_1$ dimer using the structure-fitting frame as defined by Zhang *et al.* (1996); the values in parentheses were calculated using the fitting frame defined by Baldwin & Chothia (1979).

	Human oxy (1hho)		Human deoxy (3hhb)	
	Rotation (°)	Translation (Å)	Rotation (°)	Translation (Å)
Human oxy (1hho)			13.8 (13.0)	1.7 (1.4)
Human CO met (2hco)	1.2 (1.6)	−0.4 (0.5)	14.9 (14.5)	1.3 (0.8)
Human Y state (1cmy)	11.1 (10.7)	1.2 (1.0)	23.0 (21.3)	3.1 (2.8)
Horse aquomet (2mhb)	1.3 (1.1)	0.75 (−0.01)	14.4 (12.0)	2.2 (1.1)
Goose oxy (1af4)	4.3	1.3	15.3	2.7
Goose aquomet (1c40)	3.6	1.1	14.7	2.6
Chicken oxy (1hbr)†	1.5	0.8	14.3	1.7
Greylag goose (unpublished work)	1.6	1.3	13.6	2.1

† Two residues and 169 atoms in chicken HbD are absent from the PDB coordinates because of missing electron density; therefore, they were excluded from the RMSD calculation. Chicken HbD is also excluded from the counting of residues in the subunit interface.

aquomet Hb and other Hbs are larger than those between the α-subunits.

The RMSDs between the tetramers (Table 2*b*) indicate that the quaternary structure of goose aquomet Hb is very similar to that of the goose oxy Hb, but significantly different from chicken HbD, horse aquomet Hb and human oxy Hb. The quaternary structural differences can be further characterized by the rotation angles and the translations between the two dimers. For example, the major structural difference between the T and R states of human Hb is a rotation of 12–15° and a translation of 0.8 Å for one $\alpha\beta$ dimer between the two states (Baldwin & Chothia, 1979; Perutz *et al.*, 1987). Using the $\alpha_1\beta_1$ dimer of human oxy or deoxy Hb as a template and then fitting the $\alpha_2\beta_2$ dimer, the $\alpha_2\beta_2$ dimer of goose aquomet Hb is rotated by 3.6° and translated by 1.1 Å relative to that of human oxy Hb and rotated by 14.7° and translated by 2.6 Å relative to that of human deoxy Hb (Table 2*b*). Goose oxy Hb has similar rotation angle and translation as aquomet Hb (Table 2*b*), indicating that both goose oxy and aquomet Hbs are in the R state, but are slightly different from the typical human R state. On the other hand, human CO-met Hb (2hco; Baldwin, 1980), horse met Hb, chicken oxy HbD and greylag goose oxy Hb (unpublished data) are in the typical human R state, with rotation angles and translations of 1.2° and 0.4 Å, 1.3° and 0.75 Å, 1.5° and 0.8 Å or 1.6° and 1.3 Å, respectively, relative to human oxy Hb and 14.9° and 1.3 Å, 14.4° and 2.2 Å, 14.3° and 1.7 Å or 13.6° and 2.1 Å, respectively, relative to human deoxy Hb (Table 2*b*). Obviously, the quaternary structures of both goose oxy and aquomet Hbs are significantly different from that of human Y state as in carbonmonoxy human Hb Ypsilanti (1cmy; Smith *et al.*, 1991; Table 2*b*) or cyanomet human Hb (Smith & Simmons, 1994). Therefore, the quaternary structural feature of bar-headed goose Hb is not a common feature in avian Hbs, but probably is a unique feature of bar-headed goose Hb or of Hbs from highland animals. We have named it the 'R_H' form, representing high oxygen affinity. Further studies on Hbs of other highland animals are necessary to confirm this hypothesis.

3.3. Subunit interface and the roles of four residues that differ between bar-headed goose and greylag goose Hbs

In the $\alpha_1\beta_1$ and $\alpha_1\beta_2$ interfaces, the nature and number of residues in contact in goose aquomet and oxy Hbs are generally similar to those in chicken HbD, horse aquomet Hb and human oxy Hb. However, in the $\alpha_1\alpha_2$ and $\beta_1\beta_2$ interfaces, fewer $\alpha_1\alpha_2$ contacts and many more $\beta_1\beta_2$ contacts were found in goose Hb than human and horse Hbs. The numbers of residues in contact in goose aquomet, goose oxy, horse aquomet and human oxy Hbs are 28, 44, 64 and 52, respectively, for the $\alpha_1\alpha_2$ interface, and 31, 17, 2 and 0, respectively, for the $\beta_1\beta_2$ interface. Chicken HbD was not used for this comparison since the coordinates of two residues and 169 side-chain atoms are absent in the available coordinates. This is consistent with and could be a consequence of the unique quaternary structure described above and may be related to the IPP-binding site between $\beta_1\beta_2$ subunits (see below).

The four amino-acid differences between greylag goose Hb and bar-headed goose Hb are all located on the subunit surface. Two of them, α119 and β125, are located on the $\alpha_1\beta_1$ interface, while the other two, α18 and α63, are located on the molecular surface. Changing α119 from Pro in greylag goose Hb to Ala in bar-headed goose Hb has been shown in previous studies to reduce the hydrophobic contact with Leuβ55, thereby loos-

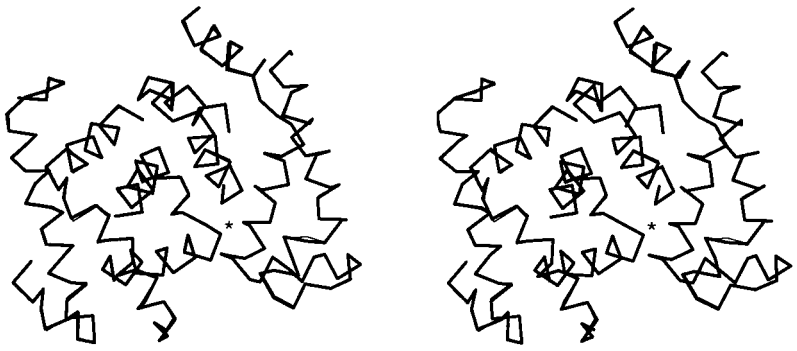

Figure 4
Alignment of the C^{α} traces of bar-headed goose aquomet Hb (thick line) with oxy Hb (thin line). The * in the figure represents the position of α119; the chain on the left is the α-subunit and that on the right is the β-subunit.

ening the $\alpha_1\beta_1$ interface (Zhang *et al.*, 1996). The aquomet Hb structure confirmed this, as the closest distance between Alaα119 and Leuβ55 (4.52 Å) is very similar to that observed in oxy Hb (4.56 Å) (Fig. 5*a*); both are too distant to make a van der Waals contact. Such a change in the $\alpha_1\beta_1$ interface might also be maintained in the goose deoxy Hb as the $\alpha_1\beta_1$ interface, also known as the packing interface, undergoes little movement during the T–R interchange, whereas the $\alpha_1\beta_2$ interface, also known as the sliding interface, undergoes significant rotational movement during the T–R interchange. Additionally, chicken HbD also has a Proα119 and a Leuβ55 as in greylag goose Hb (Table 3) and in its crystal structure Proα119 CG makes a contact with Leuβ55 CD2 at a distance of 3.88 Å (Fig. 5*a*). Therefore, greylag goose Hb may be expected to possess this van der Waals contact which is absent in bar-headed goose Hb.

In addition to α119, changing Gluβ125 in greylag goose Hb to Asp in bar-headed goose Hb may also contribute to the oxygen-affinity increase. In bar-headed goose oxyHb, Aspβ125 OG1 makes one van der Waals contact with Thrα34 CG at a distance of 3.49 Å. In aquomet Hb, the distance is 3.89 Å (Fig. 5*b*). In chicken HbD, β125 is a Glu residue as in greylag goose and is not in contact with Thrα34 or any other residues in the α-subunit. However, when Proα50 in chicken HbD is changed to Hisα50 in bar-headed goose and greylag goose Hbs, the van der Waals contact between Gluβ125 and Thrα34 is absent, but Gluβ125 OE2 is 3.80 Å from Hisα50 NE2; when Asp β125 in bar-headed goose aquomet Hb is changed to the Glu conformation in chicken HbD, the new OE2 atom is 3.77 Å from Hisα50 NE2 (Fig. 5*b*). Therefore, if the side-chain flexibility of Glu and His are considered, Gluβ125 may form a salt bridge with Hisα50 in greylag goose Hb, the interaction force of which is usually stronger than that of a van der Waals contact. This may also conceivably contribute to the higher oxygen affinity, as does the Proα119→Ala change.

Residue pairs α119–β55 and α34 (or α50)–β125 are located on two opposite edges of the $\alpha_1\beta_1$ interface, like two switches of the $\alpha_1\beta_1$ dimer (Fig. 6). Subtle loosening of the interface on both ends may increase the oxygen-binding affinity since the gap left at the $\alpha_1\beta_1$ contact raises the oxygen affinity because it relaxes the tension in the deoxy or T structure (Perutz, 1983).

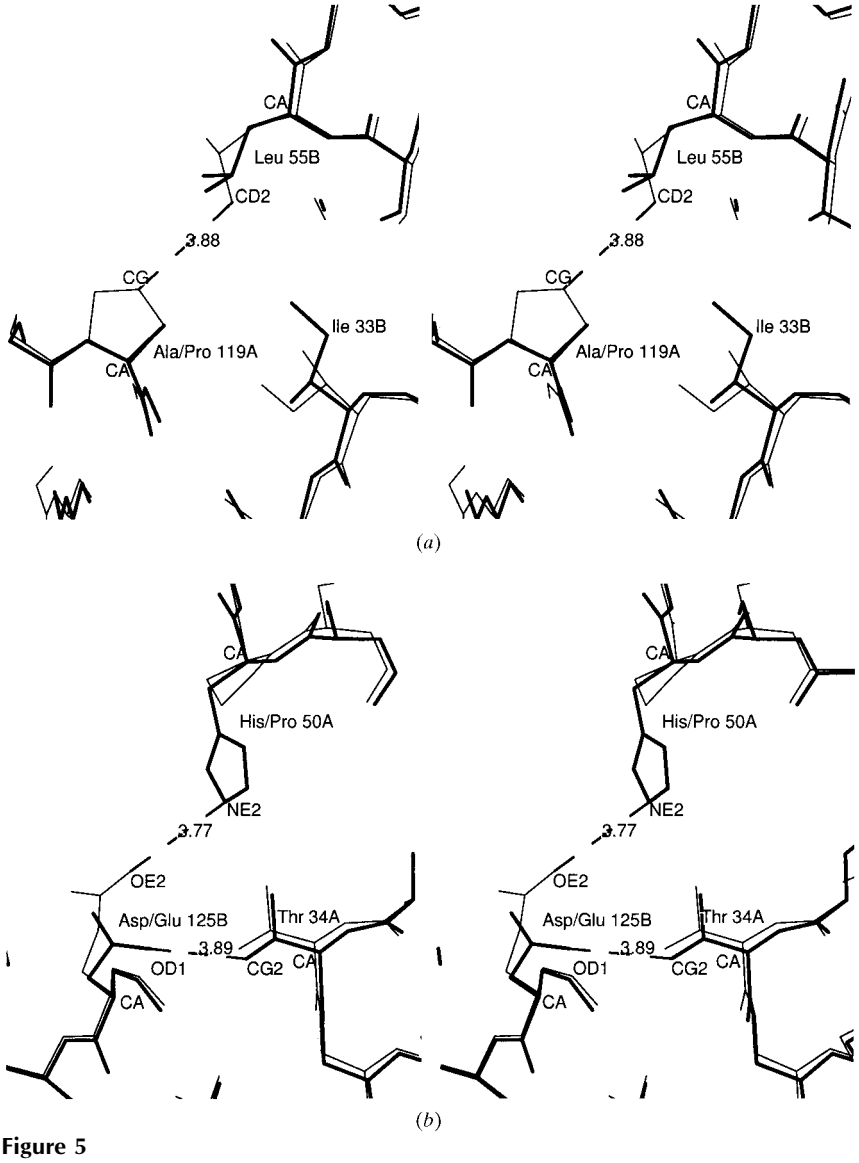

Figure 5
Close-up view of the $\alpha_1\beta_1$ interface around α119 (*a*) and β125 (*b*) in goose aquomet Hb (thick line) and chicken HbD (thin line). The two structures were superimposed based on the fitting frame defined by Zhang *et al.* (1996).

3.4. Haem- and IPP-binding sites

The geometry of the haem group in goose aquomet Hb is different from that in goose oxy Hb, since the haem iron Fe^{2+} in the oxy form is oxidized to Fe^{3+} in the aquomet form and the ligand oxygen is replaced by a water molecule, but is similar to that in horse aquomet Hb (Table 4). The residues surrounding the haem-binding pocket are the same in the goose oxy and aquomet Hbs and are similar to those in horse aquomet Hb, except that Metα32, Thrα39, Pheα46, Valα62, Pheβ45 and Lysβ66 are also involved in the haem-binding pocket of the goose aquomet Hb. In the α-subunit of the goose aquomet Hb, the side chain His45 NE2 forms a hydrogen bond with O1D of the propionate side chain in the haem at a distance of 2.79 Å (2.74 Å in horse metHb). In the β-subunit, Lys66 NZ forms a hydrogen bond with O1A of the propionate side chain in the haem with a distance of 2.95 Å (which was not seen in horse metHb). These hydrogen bonds may be very important in fixing haems in the

Table 3
Variation of amino-acid sequences for the two-residue pairs in the $\alpha_1\beta_1$ interface of avian Hbs.

All Hbs are HbA unless specified. The P_{50} values in parentheses are P_{50} for whole blood.

	α119	β55	α34 (α50)	β125	P_{50} (kPa)	Max altitude (m)
Bar-headed goose	Ala	Leu	Thr (His)	Asp	0.263 (4.46)	9 000
Greylag goose	Pro	Leu	Thr (His)	Glu	0.368 (5.20)	Sea level
Andean goose	Pro	Ser	Ile	Asp	(3.91)	6 000
Ruppell's griffon	Pro	Ile	Thr	Asp	0.39	11 300
Ruppell's griffon (A′)	Pro	Ile	Ile	Asp	0.27	11 300
Black-headed gull	Pro	Asn	Ile	Asp	N/A	N/A
Canadian goose	Pro	Leu	Val	Asp	(5.6)	Sea level
Mute swan	Pro	Leu	Ile	Asp	(5.1)	Sea level
Chicken	Pro	Leu	Thr (His)	Glu	1.36	Sea level
Chicken (D)	Pro	Leu	Thr (Pro)	Glu	1.05	Sea level

Table 4
Comparisons of haem and haem-binding geometries between goose and horse aquomet Hbs.

	Goose met		Goose oxy		Horse met	
	α	α	α	β	α	β
B factor of Fe (Å^2)	10.58	9.38	23.51	19.83	31.66	27.55
B factor of O atom in water (Å^2)	2.42	2.42			10.96	9.54
Fe—O distance (Å)	1.94	2.08	1.78	1.81	1.99	1.99
His*E*7 NE2—O distance (Å)	2.98	2.54			2.83	2.84
His*F*8 NE2—Fe distance (Å)	2.24	2.02	2.10	2.07	2.13	2.18
Fe—O—*E*7 NE2 angle (°)	122.29	129.81			128.34	120.21
*F*8 NE2—Fe—O angle (°)	180.00	166.34			180.00	180.00
RMSD from planarity (Å)†	0.123	0.124	0.157	0.120	0.001	0.001
Fe–plane distance (Å)	0.148	0.134	0.211	0.132	0.072	0.213

† The plane is defined as that passing through all haem atoms excluding the side chains and the Fe atom. Other stereochemical parameters of the goose oxy Hb haem are listed in Table 1 of Zhang *et al.* (1996).

pockets. The haem pockets of both subunits are very close to neighbouring molecules and some water molecules are near the entrance of the haem pockets. In the α-subunit, three waters form four hydrogen bonds with His58 and the haem; in the β-subunit only one such hydrogen bond is present.

The oxygen loading and unloading of Hbs is modulated by allosteric effectors such as H^+, Cl^- and organic phosphate. The main organic phosphate allosteric effector for human Hb is D-2,3-diphosphoglycerate (DPG), which binds to a positively charged pocket between the two β-subunits of deoxy Hb tetramer (Arnone, 1972). It stabilizes the T-state Hb, leading to decreased oxygen affinity and increased oxygen release in tissue. The main allosteric effector for avian Hbs is inositol-D-1,3,4,5,6 pentaphosphate (IPP) and for fish Hbs is ATP or GTP (Perutz, 1983). Although no crystal structure of IPP-bound avian Hb is currently available, the IPP-binding site could be mapped based on the structural similarity with DPG-bound human Hb. The residues surrounding the IPP-binding pocket are indentical in bar-headed goose oxy, aquomet and chicken Hbs, including Valβ1, Hisβ2, Lysβ82, Argβ104, Argβ135, Hisβ139, Argβ143, Lysβ144 and Hisβ146; these residues are clustered, carry positive charges and display similar tertiary structures in the two species (Fig. 7). Of these residues, Hisβ2 and Argβ104 may be too far away from the pocket to interact directly with IPP (Fig. 7) and Hisβ2, Argβ135 and Argβ143 appear to be variable in avian Hbs as shown in a BLAST search (Altschul *et al.*, 1997); they are not positively charged residues in some other avian Hbs, which indicates the residues at these sites might be not necessary for IPP binding.

At physiological pH, the total negative charge on IPP is larger than that on DPG and the total number of positively charged residues in the proposed IPP-binding pocket is also larger than that in the DPG-binding pocket. This might be the reason why the association constants of IPP binding to avian Hbs are larger than that of IPP and DPG binding to human Hb (Rollema & Bauer, 1979; de Bruin *et al.*, 1974). Obviously, the exact location and conformation of the IPP-binding site needs to be determined by the structure of IPP-bound Hb.

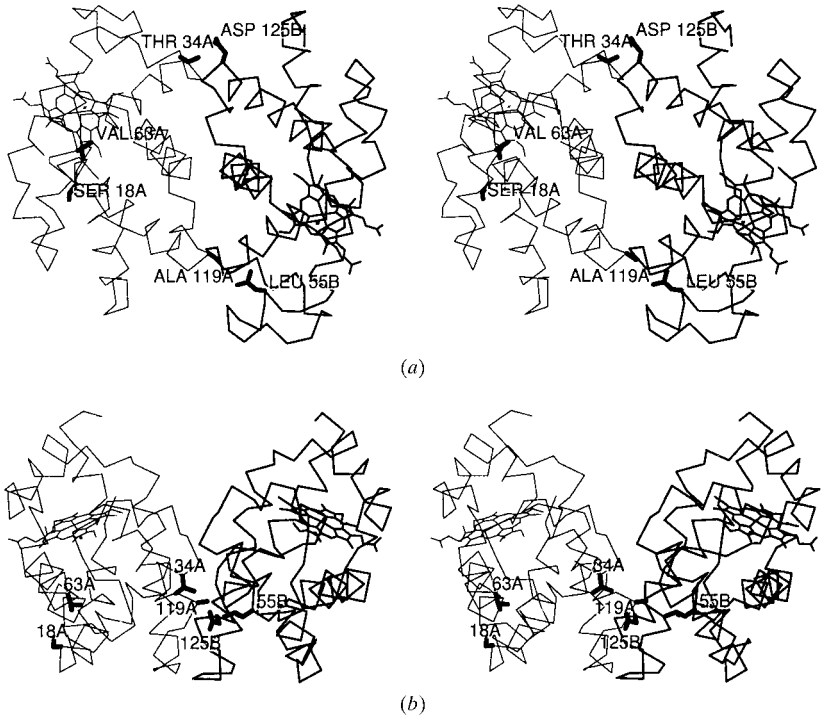

Figure 6
Residues α119 and β125 are located on two opposite edges of the $\alpha_1\beta_1$ interface. Residue pairs α119–β55 and α34 (or α50)–β125 are like two switches of the $\alpha_1\beta_1$ dimer. The thin line and thick line represent the haem group and C^α trace of the α and β subunit, respectively. The thickest lines represent the side chains of the two residue pairs. The view in (*b*) is perpendicular to that in (*a*).

4. Discussion

Birds are a class of advanced vertebrates that have evolved to adapt to flying. Their adaptation mechanism involves multiple aspects, including morphological, anatomical, physiological and molecular characteristics. For example,

birds have streamlined bodies, a feather covering, developed wings and pneumatic bones. Birds also have special lungs with airsacs which carry out double respiration. These features, common to all birds, cannot explain why some birds can adapt to extreme altitudes, however. On the other hand, at the molecular level, birds living at or migrating across high altitude were found to have Hbs with increased oxygen affinity. Structural studies of bar-headed goose Hb, therefore, may provide a clue about the molecular mechanism of the increased oxygen affinity.

Here, we show that of the four amino-acid residues that differ between the greylag goose Hb and bar-headed goose Hb, two may be neutral and the other two are located in the $\alpha_1\beta_1$ interface. Residues Proα119 and Gluβ125 in greylag goose Hb may interact with Leuβ55 and Hisα50, respectively, *via* van der Waals contacts and a salt bridge, whereas in bar-headed goose Hb these interactions are absent or weaker, resulting in fewer contacts between the two subunits and increased oxygen affinity. This appears to support the neutral theory of protein evolution, stating that the majority of mutations in a protein sequence are functionally neutral, but one or a few mutations at the critical functional sites could greatly change the protein function (Kimura, 1979).

In other avian Hbs for which the amino-acid sequences are available, the residues at or around α119, β55, α34 and β125 are also correlated with hypoxia survival abilities (Table 3). For example, the Andean goose (*Chloephaga melanoptera*, Anatidae), which lives at 6000 m altitude in the highlands of the Andes such as Peru and Bolivia, has a small residue, Ser, at position β55 of its Hb (Hiebl *et al.*, 1987). Its oxygen affinity (P_{50} of 3.91 kPa for whole blood; Jessen *et al.*, 1991) is comparable to that of the bar-headed goose (P_{50} of 4.46 kPa for whole blood and 0.263 kPa for Hb; Petschow *et al.*, 1977) and much higher than that of the greylag goose (P_{50} of 5.20 kPa for whole blood and 0.368 kPa for Hb; Petschow *et al.*, 1977). The black-headed gull (*Larus ridibundus*, Charadriiformes), which possesses adaptation to high-altitude respiration, has Proα119 and Asnβ55, which may also lack the van der Waals contact (Godovac-Zimmermann *et al.*, 1988).

However, in some avian Hbs, other residues in the $\alpha_1\beta_1$ interface may also contribute to the increased oxygen affinity. For example, Ruppell's griffon (*Gyps rueppellii*, Aegypiinae), which lives in Central Africa and can fly up to 11 300 m in altitude, has multiple Hb components, HbA, HbA′, HbD and HbD′, with a gradient of oxygen affinities (Hiebl *et al.*, 1988). The two major components, HbA and HbA′, have a P_{50} of 0.39 and 0.27 kPa, respectively. They both have a Pro at α119, an Ile at β55 and an Asp at β125, but differ at position α34 (Thr or Ile). Compared with HbA, which has a hydrogen bond between Thrα34 and Aspβ125, HbA′ has a weaker van der Waals contact between Ileα34 and Aspβ125 in the $\alpha_1\beta_1$ interface, raising its oxygen affinity. The Canadian goose (*Branta canadensis*) lives in North America and inhabits low-lying areas and is closely related to the mute swan (*Cygnus olor*), which lives in Europe and Middle Asia. The oxygen affinity of the Canadian goose (P_{50} = 5.6 kPa for whole blood) is slightly lower than that of mute swan (P_{50} = 5.1 kPa for whole blood; Oberthur, Godovac-Zimmermann *et al.*, 1982); this may also be a consequence of the different residue at α34 (Val or Ile). It was interesting to find that the residues at Proα119, Leuβ55, Thrα34 and Gluβ125 are the same in chicken HbA, HbD and greylag goose Hbs, but Hisα50 of chicken HbA, which is the same as that of greylag goose Hb, is different from Proα50 of chicken HbD; hence, the Gluβ125—α50 salt bridge may also exist in chicken HbA but not in chicken HbD. This is possibly one of the reasons why the oxygen affinity of chicken HbD is higher than that of chicken HbA (their P_{50} values are 1.053 and 1.355 kPa for HbD and HbA, respectively; Isaacks *et al.*, 1976). Therefore, the interactions between β125 and other residues in the $\alpha_1\beta_1$ interface may also affect the oxygen affinity of Hbs.

Residues in the $\alpha_1\beta_2$ interface have also been suggested to contribute to oxygen affinity, such as α38 in Ruppell's griffon HbD and HbD′ (Hiebl *et al.*, 1988) and chicken HbA and HbD (Knapp *et al.*, 1999). More extensive studies of Hb structures of various species are necessary to find the correlations between amino-acid sequences, tertiary and quaternary structures and functional characteristics such as oxygen affinity.

In the present study, we also identified a unique quaternary structure for bar-headed

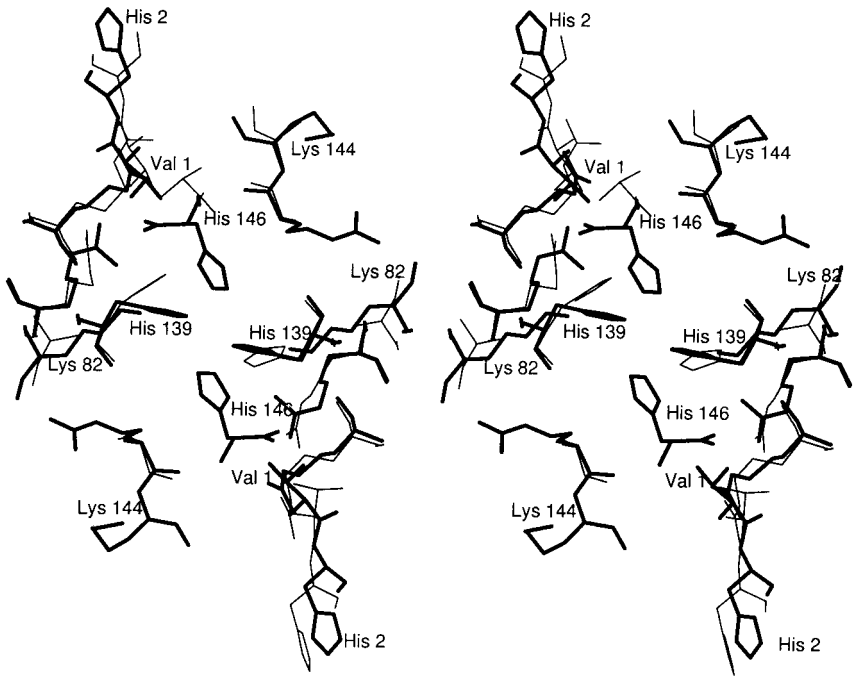

Figure 7
Potential IPP-binding site in the $\beta_1\beta_2$ interface in bar-headed goose aquomet Hb (thick line) and chicken HbD (thin line). Residues β144–146 in chicken HbD are not shown because of missing coordinates. The labelled residues (except Hisβ_2) are conserved in all bird Hbs.

goose Hb in which the relative positions of the two $\alpha\beta$ dimers in a tetramer molecule differ from that in the typical human R state and the so-called Y state. The crystals were obtained under physiological low-salt conditions, as in the cases of chicken HbD (R state) and carbonmonoxy human Hb and cynomet human Hb (Y state; Smith *et al.*, 1991; Smith & Simmons, 1994), although crystals of human oxy Hb (R state) and the horse aquomet Hb (R state) were obtained under high-salt conditions. Therefore, in disagreement with an earlier proposal (Smith & Simmons, 1994), the salt concentration is unlikely to be a determinant of the unique quaternary structure nor of the Y or R states. The unique quaternary structure is unlikely to be caused by crystal-lattice forces, as structures of human oxy Hb (R state) and horse aquomet Hb (R state) were also determined from crystals with half a tetramer in the asymmetric unit, while structures of chicken HbD (R state) and human Y state were determined from crystals with a full tetramer in the asymmetric. Therefore, we propose that the unique quaternary structure of the goose oxy and aquomet Hbs is correlated with its high oxygen affinity. We name it the 'R_H' form, representing high oxygen affinity. Structural studies of the deoxy Hb and IPP-bound fluoromet-Hb of bar-headed goose are in progress, which will certainly reveal more interesting structure–function relationships of the high-affinity Hbs.

We would like to thank Dr Matsuura for kindly providing the *AUTOMR* program and for help in the molecular-replacement calculation and Professors Xiao-Cheng Gu and Ren-Ji Zhang for many helpful suggestions. The project is supported by the National Natural Science Foundation of China.

References

Acqua, W. D., Goldman, E. R., Lin, W., Teng, C., Tsuchiya, D., Li, H., Ysern, X., Braden, B. C., Li, Y., Smith-Gill, S. J. & Mariuzza, R. A. (1998). *Biochemistry*, **37**, 7981–7991.

Altschul, S. F., Madden, T. L., Schäffer, A. A., Zhang, J., Zhang, Z, Miller, M. & Lipman, D. J. (1997). *Nucleic Acids Res.* **25**, 3389–3402.

Arnone, A. (1972). *Nature (London)*, **237**, 146–149.

Baldwin, J. M. (1980). *J. Mol. Biol.* **136**, 103–128.

Baldwin, J. M. & Chothia, C. (1979). *J. Mol. Biol.* **129**, 175–220.

Black, C. P. & Tenny, S. M. (1980). *Respir. Physiol.* **39**, 217–239.

Bruin, S. H. de, Rollema, H. S., Lambert, H. M., Van Os, J. & Van Os, G. A. J. (1974). *Biochem. Biophys. Res. Commun.* **58**, 204–209.

Brunger, A. T., Adams, P. D., Clore, G. M., DeLano, W. L., Gros, P., Grosse-Kunstleve, R. W., Jiang, J.-S., Kuszewski, J., Nilges, M., Pannu, N. S., Read, R. J., Rice, L. M., Simonson, T. & Warren, G. L. (1998). *Acta Cryst.* D**54**, 905–921.

Collaborative Computational Project, Number 4 (1994). *Acta Cryst.* D**50**, 760–763.

Godovac-Zimmermann, J., Kosters, J., Braunitzer, G. & Goltenboth, R. (1988). *Biol. Chem. Hoppe-Seyler*, **369**, 341–348.

Hiebl, I., Braunitzer, G. & Schneeganss, D. (1987). *Biol. Chem. Hoppe-Seyler*, **368**, 1559–1569.

Hiebl, I, Weber, R. E., Schneeganss, D., Kosters, J. & Braunitzer, G. (1988). *Biol. Chem. Hoppe-Seyler*, **369**, 217–232.

Howard, A. J., Nielsen, C. & Xuong, N. H. (1987). *Methods Enzymol.* **114**, 452–472.

Isaacks, R. E., Harkness, D. R., Adler, J. L. & Goldman, P. H. (1976). *Arch. Biochem. Biophys.* **173**, 114–120.

Jessen, T. H., Weber, R. E., Fermi, G., Tame, J. & Braunitzer, G. (1991). *Proc. Natl Acad. Sci. USA*, **88**, 6519–6522.

Kimura, M. (1979). *Sci. Am.* **241**, 94–104.

Knapp, J. E., Oliveira, M. A., Xiu, Q., Ernst, S. R., Riggs, A. F. & Hackert, M. L. (1999). *J. Biol. Chem.* **274**, 6411–6420.

Ladner, R. C., Heidner, E. J. & Perutz, M. F. (1977). *J. Mol. Biol.* **114**, 385–414.

Laskowski, R. A., MacArthur, M. W., Moss, D. S. & Thornton, J. M. (1993). *J. Appl. Cryst.* **26**, 283–291.

Lu, G. Y., Mao, C. H., Wei, X. C., Hua, Z. Q. & Gu, X. C. (1989). *Acta Biophys. Sin.* **5**, 259–262.

Luzzati, V. (1952). *Acta Cryst.* **5**, 802–810.

McRee, D. E. (1992). *J. Mol. Graph.* **10**, 44–46.

Matsuura, Y. (1991). *J. Appl. Cryst.* **24**, 1063–1066.

Oberthur, W., Braunitzer, G. & Kalas, S. (1981). *Hoppe-Seyler's Z. Physiol. Chem.* **362**, 1101–1112.

Oberthur, W., Braunitzer, G. & Wurdinger, I. (1982). *Hoppe-Seyler's Z. Physiol. Chem.* **363**, 581–590.

Oberthur, W., Godovac-Zimmermann, J. & Braunitzer, G. (1982). *Hoppe-Seyler's Z. Physiol. Chem.* **363**, 777–787.

Perutz, M. F. (1983). *Mol. Biol. Evol.* **1**, 1–28.

Perutz, M. F., Fermi, G., Luize, B., Shaanan, B. & Liddington, R. C. (1987). *Acc. Chem. Res.* **20**, 309–321.

Petschow, D., Wuerdinger, I., Baumann, R., Duhm, J., Braunitzer, G. & Bauer, C. (1977). *J. Appl. Physiol.* **42**, 139–143.

Ramakrishnan, C. & Ramachandran, G. N. (1965). *Biophys. J.* **5**, 909–933.

Rollema, H. S. & Bauer, C. (1979). *J. Biol. Chem.* **254**, 12038–12043.

Shaanan, B. (1983). *J. Mol. Biol.* **171**, 31–59.

Smith, F. R., Lattman, E. E. & Carter, C. W. Jr (1991). *Proteins*, **10**, 81–91.

Smith, F. R. & Simmons, K. C. (1994). *Proteins*, **18**, 295–300.

Swan, L. W. (1970). *Nat. Hist.* **79**, 68–75.

Weber, R. E., Jessen, T. H., Malte, H. & Tame, J. (1993). *J. Appl. Physiol.* **75**, 2646–2655.

Zhang, J., Hua, Z. Q., Tame, J. R. H., Lu, G. Y., Zhang, R. J. & Gu, X. C. (1996). *J. Mol. Biol.* **255**, 484–493.